

# Mechanisms of VUV Damage in BaMgAl<sub>10</sub>O<sub>17</sub>:Eu<sup>2+</sup>

Brennan Dawson,<sup>†</sup> Morgan Ferguson,<sup>†</sup> Greg Marking,<sup>‡</sup> and Anthony L. Diaz<sup>\*,†</sup>

Department of Chemistry, Central Washington University, 400 East University Way,  
Ellensburg, Washington 98926, and OSRAM SYLVANIA, Inc., Hawes Street,  
Towanda, Pennsylvania 18848

Received July 2, 2004

We have studied vacuum ultraviolet (VUV)-induced damage processes in BaMgAl<sub>10</sub>O<sub>17</sub>:Eu<sup>2+</sup> using a unique accelerated life-testing device. Emission, excitation, and reflectance spectra of doped and undoped samples before and after VUV damage reveal two independent mechanisms of degradation. The observed color shift in damaged materials is due to the migration of Eu<sup>2+</sup> ions to metastable sites in the lattice. The observed loss of brightness is due in part to the formation of color centers in the spinel layer that act as energy traps and also absorb the exciton emission of the host lattice, thus interrupting the transfer of energy from the host to the activator. Several modes of energy transfer to Eu<sup>2+</sup> are available depending on the excitation energy.

## Introduction

The development of plasma display (PDP) technology has led to significant research activity into the vacuum ultraviolet (VUV) optical properties of luminescent materials. PDPs utilize a Xe plasma discharge as the source of photoexcitation of red, green, and blue phosphors. This discharge generates photons at 147 and 172 nm, energies that are greater than the band gap of the phosphor host oxides. The blue phosphor, BaMgAl<sub>10</sub>O<sub>17</sub>:Eu<sup>2+</sup> (BAM), has been of particular interest because it is considerably less stable than the red and green emitters, both during panel fabrication (thermal damage) and panel operation (VUV damage). These phenomena have been documented in numerous publications.<sup>1–11</sup> While the thermal damage in these materials has been reasonably assigned to the oxidation of Eu<sup>2+</sup> to Eu<sup>3+</sup>, the mechanisms of VUV damage have remained somewhat more mysterious. Part of the difficulty is that many of the VUV damage studies have been conducted using functioning panels, or through long exposures to VUV radiation from discharge tubes that do not reproduce the magnitude of the photon fluxes seen in displays. This has made the systematic study of VUV

damage more challenging. Recently, we reported on a custom-built accelerated life-testing device.<sup>1</sup> With this instrument, powders are directly exposed to an intense Xe discharge and can then be removed for spectroscopic characterization. Reported here are the results of such a study on VUV damage processes in doped and undoped BAM.

BAM crystallizes in the space group *P6<sub>3</sub>/mmc*. The structure consists of MgAl<sub>10</sub>O<sub>16</sub> units separated by planes of Ba–O.<sup>12</sup> Eu<sup>2+</sup> substitutes for Ba atoms in the cation plane. The MgAl<sub>10</sub>O<sub>16</sub> units are referred to as spinel blocks: they have the MgAl<sub>2</sub>O<sub>4</sub> spinel structure with a high degree of substitution of Al<sup>3+</sup> for Mg<sup>2+</sup>, resulting in considerable defect formation.<sup>12,13</sup> In general, BAM that has been exposed to VUV radiation exhibits both a color shift and a loss of brightness. The color shift takes place because of the formation of a long-wavelength shoulder on the usual emission peak at 450 nm. Researchers generally agree that this shift must be the result of migration of Eu<sup>2+</sup> ions to metastable sites in the cation layer.<sup>1–6</sup> Several groups have shown that Eu<sup>2+</sup> can occupy two or three distinct emission centers in the lattice.<sup>13–16</sup> The specific assignment of these centers is still debated. It appears that the primary center is the Beevers–Ross position normally occupied by Ba. Other potential locations for Eu<sup>2+</sup> include the anti-Beevers–Ross site, mid-oxygen sites, and sites near defects related to those seen in Ba<sub>0.75</sub>Al<sub>11</sub>O<sub>17.25</sub>.

Much less certain thus far is the mechanism behind the loss of brightness in these materials. It has been suggested that the new Eu<sup>2+</sup> centers are less efficient,<sup>2,3</sup>

\* Corresponding author. E-mail: diaza@cwu.edu.

<sup>†</sup> Central Washington University.

<sup>‡</sup> OSRAM SYLVANIA, Inc.

(1) Howe, B.; Diaz, A. L. *J. Lumin.* **2004**, *109*, 51.

(2) Zhang, S.; Hou, Y.; Fujii, H.; Onishi, T.; Kokubu, M.; Obata, M.; Tanno, H.; Kono, T.; Uchiike, H. *J. Appl. Phys.* **2003**, *42*, 477.

(3) Zhang, S.; Kokubu, M.; Fujii, H.; Uchiike, H. *J. SID* **2002**, *10/1*, 25.

(4) Zhang, S.; Kokubu, M.; Fujii, H.; Uchiike, H. *SID Digest* **2001**, 414.

(5) Ushirozawa, M. *SID Digest* **2000**, 224.

(6) Jüstel, T.; Nikol, H. *Adv. Mater.* **2000**, *12*, 527.

(7) Zhang, S.; Kono, T.; Ito, A.; Yasaka, T.; Uchiike, H. *J. Lumin.* **2004**, *106*, 39.

(8) Diaz, A. L.; DeBoer, B. G.; Chenot, C. F. *19th Int. Disp. Res. Conf. Proc.* **1999**, 65.

(9) Kim, K.-B.; Koo, K.-W.; Cho, T.-Y.; Chun, H.-G. *Mater. Chem. Phys.* **2003**, *80*, 682.

(10) Yokota, K.; Zhang, S.; Kimura, K.; Sakamoto, A. *J. Lumin.* **2001**, *92*, 223.

(11) Kwon, T. H.; Kang, M. S.; Kim, J. P.; Kim, G. J. *Asia Display* **2001**, 1051.

(12) Iyi, N.; Inoue, Z.; Kimura, S. *J. Solid State Chem.* **1986**, *61*, 236.

(13) Pike, V.; Patraw, S.; Diaz, A. L.; DeBoer, B. G. *J. Solid State Chem.* **2003**, *173*, 359.

(14) Boolchand, P.; Mishra, K. C.; Raukus, M.; Ellens, A.; Schmidt, P. C. *Phys. Rev. B* **2002**, *66*, 134429.

(15) Mishra, K. C.; Raukus, M.; Ellens, A.; Johnson, K. H. *J. Lumin.* **2002**, *96*, 95.

(16) Ellens, A.; Zwaschka, F.; Kummer, F.; Meijerink, A.; Raukus, M.; Mishra, K. J. *Lumin.* **2001**, *93*, 147.

that photooxidation of  $\text{Eu}^{2+}$  to  $\text{Eu}^{3+}$  takes place,<sup>5,6</sup> or that other defects form in the host.<sup>25</sup> A recent study of undoped material revealed that part of the host-to-activator energy transfer in BAM under VUV excitation occurs via a host lattice emission centered at 265 nm.<sup>1</sup> Given this, we have chosen to study the VUV damage characteristics of BAM at a variety of  $\text{Eu}^{2+}$  concentrations, including the undoped host. The results of this work indicate that the disruption of energy transfer is one of the essential mechanisms of brightness loss in these phosphors.

### Experimental Section

VUV excitation and emission spectra were acquired using a standard spectrometer setup from Acton Research Corp., which utilizes a deuterium lamp as the excitation source. The lamp, monochromator, and sample chamber are evacuated to  $\sim 3.0 \times 10^{-5}$  mbar using a dry diaphragm/turbo pumping station. Excitation spectra are corrected using a sodium salicylate standard, while emission spectra between 300 and 800 nm are corrected using a NIST calibrated standard lamp. The procedure used for correcting emission spectra between 190 and 300 nm is described in ref 1. A separate correction procedure is required because a different grating is used at these wavelengths and no standard lamp is available. Reflectance spectra between 190 and 300 nm were acquired on a Perkin-Elmer 330 equipped with a  $\text{BaSO}_4$ -coated integrating sphere. This system uses a deuterium lamp for wavelengths between 200 and 350 nm, and a tungsten lamp for wavelengths longer than 350 nm. The accelerated VUV life-testing device is described in ref 1 and is comprised of a 100 cm rectangular loop of 5 cm i.d. Pyrex tubing with sidearm sample introduction, gas inlet, and pumping ports. An intense discharge is generated inside the tube using 20 mTorr flowing Xe. Powder samples on 4 cm Macor disks are placed inside the tube, and the discharge is operated for 1–8 h. Phosphors in the chamber are directly exposed to the Xe discharge. In general, hundreds of hours of panel damage are simulated in only a few hours.

$\text{Ba}_{1-x}\text{MgAl}_{10}\text{O}_{17}:\text{Eu}_x$  samples were prepared by wet ball-milling blends of  $\text{BaCO}_3$ ,  $\text{Al}(\text{OH})_3$ ,  $\text{MgO}$ , and  $\text{Eu}_2\text{O}_3$ , with a small amount of  $\text{BaF}_2$  used in place of  $\text{BaCO}_3$  as a reaction aid. The samples were twice fired for 3 h in open alumina crucibles under a 75%  $\text{H}_2$ /25%  $\text{N}_2$  flow at 1650 °C, with milling between firing steps. Samples were analyzed by glow discharge mass spectroscopy to check that no F was retained. All samples were determined to be single-phase by powder X-ray diffraction.

### Results and Discussion

**Color Shift from VUV Damage.** Figures 1 and 2 show the effects of VUV damage on the emission spectra of  $\text{Ba}_{1-x}\text{MgAl}_{10}\text{O}_{17}:\text{Eu}_x$  doped at 1% and 10% Eu, respectively. In each case, the exposure time in the life-testing chamber was 4 h. Note that the data are

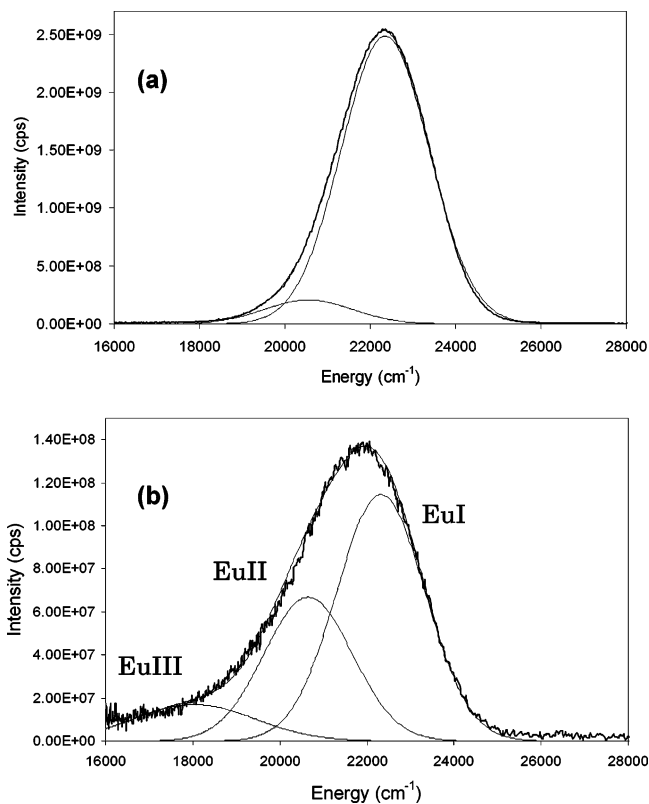


**Figure 1.**  $\text{Ba}_{0.99}\text{MgAl}_{10}\text{O}_{17}:\text{Eu}_{0.01}$ : (a) fresh and (b) after 4 h in the accelerated life-testing chamber.

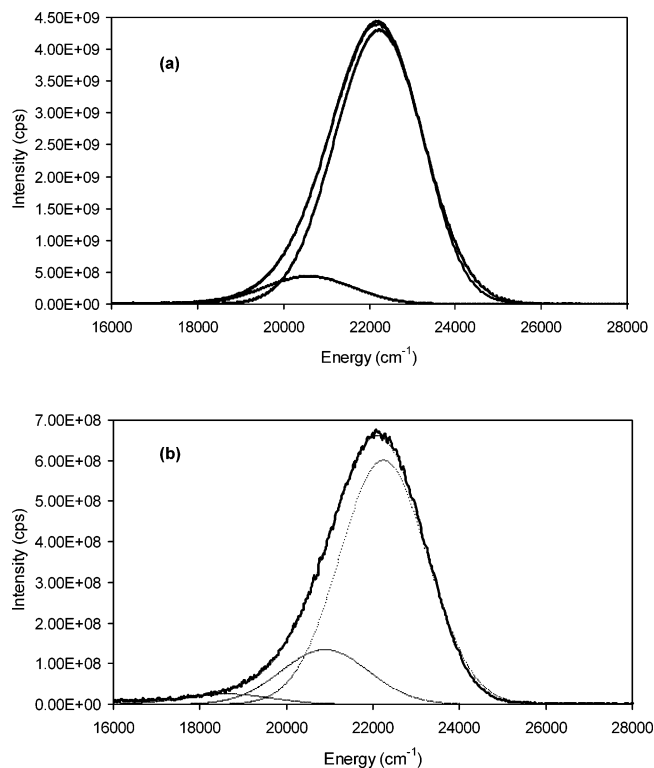


**Figure 2.**  $\text{Ba}_{0.90}\text{MgAl}_{10}\text{O}_{17}:\text{Eu}_{0.10}$ : (a) fresh and (b) after 4 h in the accelerated life-testing chamber.

presented on an energy scale. After the VUV damage, the sample doped at 10% Eu decreases to about 16% of the integrated brightness of the fresh sample, while the sample doped at 1% Eu decreases to about 8% of fresh. Our observation that the sample with higher  $\text{Eu}^{2+}$  loading is relatively more stable to VUV damage is

(17) Zachau, M.; Schmidt, D.; Meuller, U.; Chenot, C. F. World Patent WO 99/34 389, 1999.

(18) Wu, Z.; Cormack, A. N. *J. Electroceram.* **2003**, *10*, 179.

(19) Smyth, D. M. *The Defect Chemistry of Metal Oxides*; Oxford University Press: Oxford, 2000; Chapter 2.

(20) Mishra, K. C.; DeBoer, B. G.; Schmidt, P. C.; Osterloh, I.; Stephan, M.; Eyert, V.; Johnson, K. H. *Ber. Bunsen-Ges. Phys. Chem.* **1998**, *102*, 1772.

(21) Mishra, K. C.; Osterloh, I.; Anton, H.; Hannebauer, B.; Schmidt, P. C.; Johnson, K. H. *J. Mater. Res.* **1997**, *12*, 2183.

(22) Lushchik, A.; Kirm, M.; Kotlov, A.; Liblik, P.; Lushchik, Ch.; Maaros, A.; Nagirnyi, V.; Savikhina, T.; Zimmerer, G. *J. Lumin.* **2003**, *102–103*, 38.

(23) Jüstel, T.; Krupa, J.-C.; Weichert, D. U. *J. Lumin.* **2001**, *93*, 179.

(24) Hirakawa, Y.; Nakamura, K.; Imasaka, T. *Anal. Chem.* **2001**, *73*, 5472.

(25) Kim, K.-B.; Kim, Y.-I.; Chun, H.-G.; Cho, T.-Y.; Jung, J.-S.; Kang, J.-G. *Chem. Mater.* **2002**, *14*, 5045.

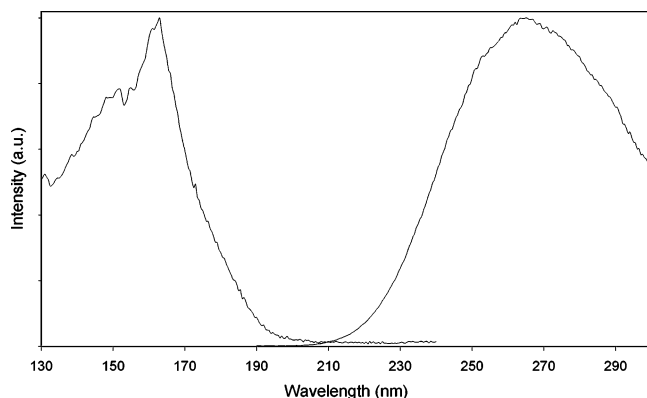


**Figure 3.** Normalized excitation ( $\lambda_{\text{em}} = 265$ ) and emission ( $\lambda_{\text{ex}} = 160$  nm) spectra of  $\text{BaMgAl}_{10}\text{O}_{17}$ .

consistent with what has been reported by several other groups.<sup>3,6,17</sup> Note that the 10% Eu sample is more stable with respect to both color (spectral shape) and efficiency. Measurements we performed on samples doped at 5% Eu (not shown) are also consistent with this trend. The excitation wavelength in these spectra is 147 nm. In an operating panel, the Xe discharge consists of a peak at 147 and a broad band centered around 172 nm. VUV damaged samples experience a greater loss of excitation efficiency at 147 nm than at 172 (refs 1,5 and Figure 3); therefore, our measured brightness loss is lower than what would be observed in a display by a factor of about 2. Note that at each concentration VUV damage induces the formation of a low energy (long wavelength) tail on the emission spectrum.

The spectra in Figures 1 and 2 have been fit using Gaussian profiles to approximate emission from the various activator centers. This technique has been used effectively with  $\text{Sm}^{2+}$ - and  $\text{Eu}^{2+}$ -doped barium magnesium aluminates as a means of elucidating the number and nature of activator sites in these compounds,<sup>13,16</sup> although one has to be careful about how the fitting is done. Where possible, the number of Gaussians that are used should be based on some other knowledge of the expected number of emission centers. In addition, the least-squares minima in parameter space tend to be broad, shallow wells; that is, a number of possible solutions exist that will yield reasonable fits. Therefore, restrictions must also be placed on the fitting parameters. In the case of  $\text{BaMgAl}_{10}\text{O}_{17}:\text{Eu}^{2+}$ , there is general agreement that there are at least two  $\text{Eu}^{2+}$  sites, and some researchers have argued that there are three. Pike et al. found that the emission of fresh, stoichiometric BAM:Eu can be fit with three Gaussians, but the authors also pointed out that the spectrum can be effectively fit with two.<sup>13</sup> Peak fitting of  $\text{Sm}^{2+}$  emission spectra also indicated two emission centers in BAM.<sup>16</sup> However, theoretical fitting of excitation spectra,<sup>15</sup> as well as  $^{151}\text{Eu}$  Mössbauer spectroscopy,<sup>14</sup> have indicated the possibility of three unique sites for  $\text{Eu}^{2+}$ . Typically, the primary emission center is assigned to  $\text{Eu}^{2+}$  on the normal Ba site (the Beevers–Ross site in the cation layer), while the second center is assigned to  $\text{Eu}^{2+}$  on the anti-Beevers–Ross site. These centers are labeled EuI (22 100  $\text{cm}^{-1}$ ) and EuII (20 200  $\text{cm}^{-1}$ ), respectively, in Figure 1b. The third center, when proposed, has been assigned alternatively to  $\text{Eu}^{2+}$  in the spinel block, to  $\text{Eu}^{2+}$  on mid-oxygen sites in the cation layer, or to  $\text{Eu}^{2+}$  associated with defect centers in the lattice. We believe

that there is a third metastable site for  $\text{Eu}^{2+}$  in this host, but that it is not significantly populated in the fresh sample.

For the spectra shown here, we first modeled the emission of the fresh samples using two Gaussians, with the requirement that the two peak widths be equal. Although we would not necessarily expect the two emission centers to have identical peak widths, the coordination environments are quite similar for the Beevers–Ross and anti-Beevers–Ross sites in the cation plane. Thus, this requirement reasonably reduces the number of possible solutions. Spectra after VUV damage were fit by adding a single new peak to the low energy side of the emission (EuIII at 17 900  $\text{cm}^{-1}$  in Figure 1b). The intensities of the two primary peaks were allowed to vary, but not their widths or positions. The parameters we obtain for the third emission center are essentially identical for any initial Eu concentration, with the EuIII peak being somewhat broader than the other two. Interestingly, we note that this new center is nearly identical to what was found in peak fitting done on  $\text{Eu}^{2+}$ -doped  $\text{Ba}_{0.75}\text{Al}_{11}\text{O}_{17.25}$  (BAL).<sup>13</sup> In that case, although it was clear that this center must be associated with the defects formed in going compositionally from BAM to BAL, it could not be determined whether the site was related to  $\text{Al}^{3+}$  vacancies in the host, or to Al–O–Al bridges that form in the lattice as  $\text{Al}_2\text{O}_3$  is substituted for MgO.

A summary of the spectral data is provided in Table 1. Along with an overall decrease of brightness in these materials, the data suggest a migration of  $\text{Eu}^{2+}$  out of the primary site and into the sites labeled EuII and EuIII. This is evidenced by a shifting in the relative populations of the sites after VUV damage. Note from Table 1 that relatively more migration is observed in the material doped at 1% Eu. We believe that the data support a model in which the EuIII site is an inherent property of the host-lattice (i.e., not a site created during damage) and that there are a limited number of these sites available for occupation by Eu. This site may be associated with Al–O–Al bridges or some other randomly occurring lattice defect, or it may be a unique site near the surface, but we do not believe it is a position like the mid-oxygen site, which is available in every unit cell. If the EuIII site were in every unit cell, then we would expect the Eu migration to follow first-order kinetics. That is clearly not the case here, because the EuIII/EuI ratio depends on the initial concentration of Eu (whereas it should be independent of the initial concentration in a first-order model). The data are more consistent with the idea that there are a small fraction of these defect sites in the host, and they are populated during Eu migration. The EuIII/EuI ratio is then higher in the sample doped at 1% Eu because the absolute number of EuIII sites represents a larger fraction of the total Eu concentration than it does at 10% Eu. Finally, we note that at 5% Eu (not shown), the observed EuIII/EuI ratio in the VUV-damaged material is between those values obtained at 1% and 10% Eu. To further clarify this model, we considered the integrated areas of the EuIII peak in both damaged samples. If the area of the EuIII peak is corrected for the absolute difference in brightness between the 1% and 10% Eu samples, one finds that the population of EuIII sites in the two damaged samples is nearly identical (it will be pointed



Table 1. Summary of Peak Fitting on Fresh and VUV-Damaged BaMgAl<sub>10</sub>O<sub>17</sub>:Eu

	color			EuI	EuII	EuIII
	x	y				
10% Eu – fresh	0.147	0.049	peak area	$1.11 \times 10^{13}$	$1.13 \times 10^{12}$	
			% of total	90.8%	9.2%	
VUV damaged			peak area	$1.55 \times 10^{12}$	$3.46 \times 10^{11}$	$7.18 \times 10^{10}$
			% of total	78.7%	17.6%	3.7%
1% Eu – fresh	0.150	0.043	peak area	$6.40 \times 10^{12}$	$5.28 \times 10^{11}$	
			% of total	92.4%	7.6%	
VUV damaged			peak area	$3.11 \times 10^{11}$	$1.59 \times 10^{11}$	$4.57 \times 10^{10}$
			% of total	60.3%	30.9%	8.9%

out in the next section that the loss of brightness is not related to the migration of Eu<sup>2+</sup> in these materials). Again, this implies that there are a fixed number of EuIII sites available in the BAM lattice and that the energetic barrier to migration is small.

The nature of the metastable site remains uncertain. Wu and Cormack have used theoretical calculations to model a variety of potential defects in BAM.<sup>18</sup> They found that Ba interstitials (Frenkel defects) were the lowest energy defect, followed by several types of oxygen interstitials. These oxygen interstitials place additional O atoms in the cation layer and include the Al–O–Al bridges (called Reidinger defects) that are found in Ba<sub>0.75</sub>Al<sub>11</sub>O<sub>17.25</sub>. This is noteworthy, because our peak fitting data indicate that the EuIII emission center is very similar to the Eu emission center associated specifically with Ba<sub>0.75</sub>Al<sub>11</sub>O<sub>17.25</sub>.<sup>13</sup> In any crystalline lattice, even one synthesized under ideal conditions, free energy considerations dictate that there will be some concentration of defects. The concentration will depend on the balance between the enthalpic cost of forming the defect and the gain in entropy created by its formation.<sup>19</sup> This will create local metastable sites in the host that are not available in every unit cell. Our inclination, therefore, is to associate the EuIII site with Reidinger-type defects in this lattice. The authors recognize this as a best estimate based on current data. For example, the EuIII site could be related to unique positions near the surface of the crystal.

**Energy Transfer in Ba<sub>1-x</sub>MgAl<sub>10</sub>O<sub>17</sub>:Eu<sub>x</sub>.** To understand the various mechanisms of efficiency degradation, it is first necessary to describe the processes of host-to-activator energy transfer at work in BAM. Howe and Diaz have recently reported that an efficient host lattice emission at 265 nm from undoped BAM is responsible for a significant fraction of the energy transfer in the doped phosphor.<sup>1</sup> They argued that the emission comes from a self-trapped exciton (STE) at Ba–O groups and proposed that excitation near the band edge at 190 nm takes place into Ba 5d levels, while excitation at higher energy takes place in the spinel layer. This model is based partly on theoretical modeling of BaO<sub>9</sub> clusters in BAM.<sup>15</sup> It is also generally consistent with the results of band structure calculations on other oxide systems that are comprised of an anionic framework and a basic oxide. In a study on Ba, Y, and Lu borates, for example, it was found that the valence band is comprised primarily of B<sub>x</sub>O<sub>y</sub> bonding states, while the lowest energy portion of the conduction band consists largely of metal d states.<sup>20</sup> The antibonding B<sub>x</sub>O<sub>y</sub> levels occur at slightly higher energy. Similar results were found from calculations on LaPO<sub>4</sub>.<sup>21</sup> In this case, the authors note that the La d contribution is significant near the band edge and that this may lead to localiza-

tion of an electron–hole pair upon excitation of the host. We propose, then, that states near the band edge in BAM are comprised primarily of Ba 5d, while states at higher energies are antibonding states from the spinel (MgAl<sub>10</sub>O<sub>16</sub>) framework. In this case, the observed emission is assigned to excitons trapped locally at Ba 5d states. Lushchik et al. reported on host lattice emission from BaMgAl<sub>10</sub>O<sub>17</sub> and SrMgAl<sub>10</sub>O<sub>17</sub> (SAM).<sup>22</sup> They assigned the emission to the recombination of electrons in the conduction band with holes trapped near Mg<sup>2+</sup> ions. Although they did not comment specifically on the nature of the excited state, they proposed that excitation into the spinel block of SAM takes place at energies 2 eV greater than the band edge. Of course, any modeling of these systems would be greatly aided by more detailed band structure calculations.

Excitation and emission spectra of undoped BAM are shown in Figure 3. The spectra reveal that the host emission is most efficient for excitation right near the band edge, peaking at about 163 nm. At 130 nm, the efficiency of excitation has decreased by about 50%. Thus, excitation directly at the Ba–O groups readily forms an STE, while excitation into the spinel block requires an energy-transfer step to Ba and is therefore less efficient. Interestingly, we note that the excitation spectrum for the host emission does not match the absorption spectra of the doped or undoped hosts. Such data have been reported previously<sup>13,23</sup> and show essentially flat absorption between 120 and 180 nm before dropping off at the band edge. This again implies that, although the same number of photons is absorbed at 130 and 163 nm, the quantum efficiency of the host emission is about 50% lower for excitation at 130 nm.

The excitation spectrum in Figure 3 also does not match that of the Eu<sup>2+</sup> emission in doped samples. Excitation spectra for a series of BAM samples doped at 1%, 5%, and 10% Eu<sup>2+</sup> are shown in Figure 4. The spectra can be roughly divided into two parts: a host lattice excitation region for wavelengths shorter than 200 nm, and a direct Eu<sup>2+</sup> excitation region for wavelengths longer than 200 nm. As the Eu concentration increases, the overall intensity increases, as expected. In addition, short wavelength excitation generates more emission than long wavelength excitation at low Eu concentrations, presumably because of the high absorption cross section of the host. At 10% Eu, the relative emission intensities in the two regions are about the same. Hirakawa et al. have made similar observations.<sup>24</sup> Two additional features should be noted in these data. The first is that the excitation spectra in the host lattice region do not match the spectrum of Figure 3, as has been noted. Second, the intensity between 160 and 180 nm is slightly greater than the intensity at shorter

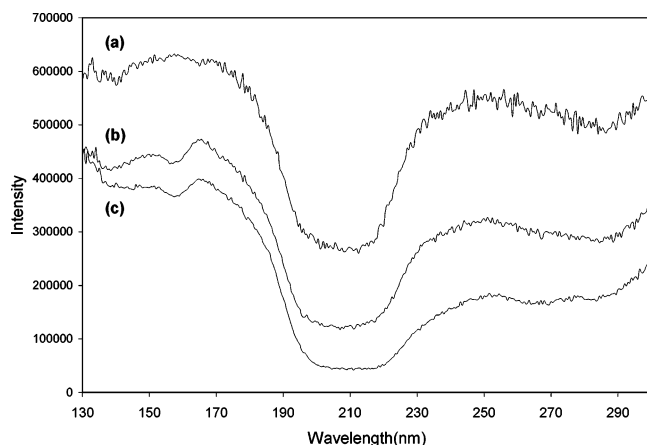


**Figure 4.** Excitation spectra of  $\text{Ba}_{1-x}\text{MgAl}_{10}\text{O}_{17}:\text{Eu}_x$  for (a)  $x = 0.10$ , (b)  $x = 0.05$ , and (c)  $x = 0.01$ .

wavelengths for 1% and 5% Eu, while the spectrum is fairly flat for 10% Eu.

These data indicate that (a) there are nonradiative energy-transfer pathways to  $\text{Eu}^{2+}$  in addition to the radiative mechanism and (b) the fraction of energy transferred radiatively versus nonradiatively is greater for excitation in the 160 nm region (into the Ba states) than for excitation in the 140 nm region (into spinel states). This second conclusion comes from the fact that the emission intensity from  $\text{Eu}^{2+}$  is essentially the same in these two regions, while the intensity of the host lattice emission is not.

By comparing the integrated intensity of the host lattice emission to the integrated intensity of the  $\text{Eu}^{2+}$  emission at a 10% loading, we estimate that at 163 nm 41% of the energy transfer takes place via the STE emission. At 130 nm, 21% of the energy transfer is radiative. These calculations were made using the 10% Eu sample because by this loading no emission from the host lattice is detected and the VUV-excited intensity is saturated.<sup>1,25</sup> Our estimate is complicated by the fact that our system uses different gratings for emission from 190 to 300 nm than for emission from 250 to 1000 nm. The host emission is split between these two ranges, so that it was necessary to compare the intensity in the region of overlap to make an estimate of the total photon flux. In addition, glow discharge mass spectrometry of our undoped samples indicated the presence of about 120 ppm  $\text{Eu}^{2+}$ , which may result in a slight underestimation of the emitted photon flux from the host. However, we believe the values presented here are a very good approximation of the distribution of energy transfer in this system. Because radiative transfer only accounts for 41% of the energy under 163 nm, there must be other means for  $\text{Eu}^{2+}$  to capture this energy. We also expect that direct excitation of  $\text{Eu}^{2+}$  is also taking place at excitation wavelengths between 170 and 200 nm.

It seems that there are two reasonable possibilities for accounting for the nonradiative energy transfer to  $\text{Eu}^{2+}$  under excitation at 147 nm, which appears to be relatively more efficient than transfer to Ba states. It is possible that excitation takes place directly into high-lying  $4f^7$  states of  $\text{Eu}^{2+}$ . To our knowledge, there are no theoretical or experimental data relating the energetic positions of the  $4f^7$  excited states of  $\text{Eu}^{2+}$  to the  $^8\text{S}$  ground term beyond the UV. The most relevant data come from the work of Wegh et al., who identified the

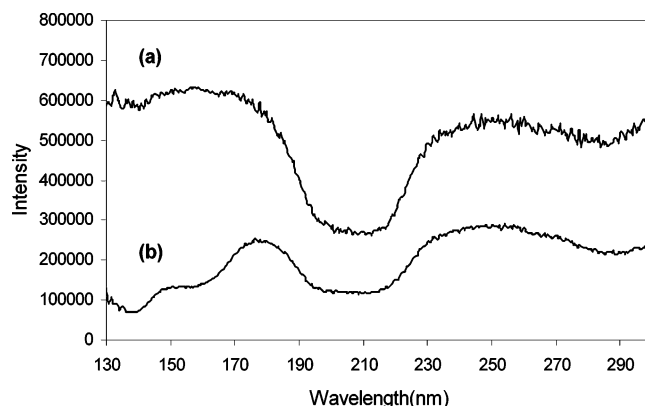


**Figure 5.** Excitation spectra of  $\text{Ba}_{0.9}\text{MgAl}_{10}\text{O}_{17}:\text{Eu}_{0.1}$ : (a) fresh sample and (b) after 4 h in the VUV life-testing chamber.

energies of  $4f^7$  terms in isoelectronic  $\text{Gd}^{3+}$ .<sup>26</sup> In this case, there were terms as high as  $66\,000\text{ cm}^{-1}$  (about 150 nm) above the ground state, but the absorption intensities were fairly weak. It seems more likely that there is a relatively efficient mechanism for  $\text{Eu}^{2+}$  to trap an electron excited into the spinel states of the host and that this mechanism is not available to Ba in this lattice. Indeed, the transfer may involve high-lying  $4f^7$  states, but with our current data we have no means of clarifying this process. From the spectra of Figure 4, it does appear that excitation through the spinel block becomes relatively more efficient as more Eu is added to the host.

**Loss of Efficiency from VUV Damage.** It is unlikely that the dramatic decrease in the overall brightness of these materials is the direct result of the observed migration of Eu (or Ba) ions discussed previously. While we might expect some differences in the quantum efficiency of  $\text{Eu}^{2+}$  at various locations in the cation layer, it seems improbable that this difference would be as high as 70% or 80%. We believe, therefore, that the spectral shift and the loss of efficiency are observations that stem from two distinct phenomena. In fact, other research groups have proposed that the primary mechanism of VUV damage is probably related to the host and not the  $\text{Eu}^{2+}$  activator.<sup>7,27</sup> The effects of VUV damage on the emission of the undoped host,  $\text{BaMgAl}_{10}\text{O}_{17}$ , are similar to what is seen in doped materials. There is a dramatic decrease in the emission intensity, with the relative magnitude of the decrease being about 10% greater than what is observed in Eu-doped samples damaged under the same conditions. From these data, it has been proposed that a significant portion of the observed loss of efficiency in doped materials is caused by degradation of the host lattice emission, resulting in disruption of the radiative host-to-lattice energy-transfer mechanism.<sup>1</sup> We have reproduced the results on undoped samples, but, as the spectra are essentially identical to those that have been published, they are not shown here. The fact that the host emission is damaged somewhat more than the  $\text{Eu}^{2+}$  emission provides further evidence that other mechanisms of transfer to  $\text{Eu}^{2+}$  are available.

Figure 5 shows the excitation spectrum of BAM:10% Eu before and after 4 h in the VUV life-testing chamber.

(26) Wegh, R. T.; Meijerink, A.; Lamminmäki, R.-J.; Hölsä, J. *J. Lumin.* **2000**, 87–89, 1002.

(27) Moine, B.; Bizarri, G. *Mater. Sci. Eng.* **2003**, B105, 2.

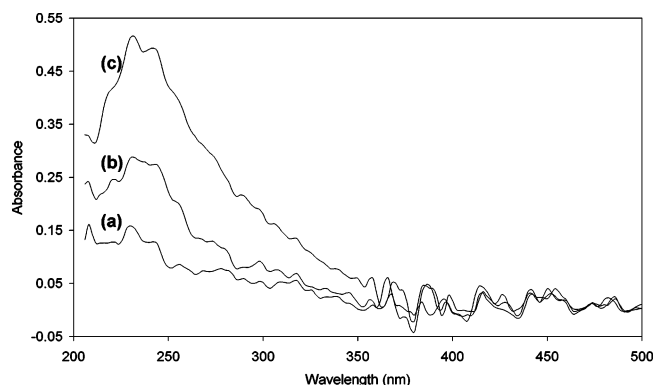


**Figure 6.** Diffuse reflectance spectra of undoped  $\text{BaMgAl}_{10}\text{O}_{17}$ , converted to an absorbance scale. Sample (a) was exposed to approximately 2 h of VUV irradiation in our spectrometer, while sample (b) was exposed to approximately 10 h of irradiation. The sample in (c) was placed in the VUV life-testing chamber for 8 h.

The emission wavelength is 450 nm. The spectra are similar to what has been reported elsewhere for VUV-damaged BAM.<sup>1,5</sup> Note that the relative loss of efficiency from VUV damage is fairly uniform for excitation between 170 and 300 nm, but that it is more severe at wavelengths shorter than this. Thus, it appears that the nonradiative transfer to  $\text{Eu}^{2+}$  through the spinel layer has been disrupted more severely than the other modes of excitation. Any model of VUV damage in this phosphor must therefore take into account the apparent decreased efficiency of the STE emission, which may involve Ba–O groups, as well as the formation of some kind of defect within the spinel block. In addition, note that the efficiency of the  $\text{Eu}^{2+}$  emission has also decreased even under direct excitation at wavelengths longer than about 210 nm. This is interesting because that process does not involve the host lattice.

We have found that the majority of these observations can be assigned to the formation of electronic defects, primarily within the spinel portion of the host. This can be seen in Figure 6, in which diffuse reflectance spectra of undoped  $\text{BaMgAl}_{10}\text{O}_{17}$  after varying degrees of VUV damage are compared. For these measurements, fresh undoped BAM that had never been exposed to VUV radiation (either in the life-testing instrument or in our spectrometer) was used as a standard. The y-axis has been converted to an absorbance scale. Two of the samples were exposed to different amounts of VUV irradiation during measurements in our spectrometer, while a third sample was more severely damaged directly in the VUV life-testing chamber. It can be seen that a broad absorption center forms with a peak at about 235 nm that becomes more pronounced with longer exposures. This new absorption band exhibits excellent overlap with the exciton emission and provides a means of diverting this emission away from Eu atoms in the doped host. Moine and Bizarri have also proposed that VUV damage could disrupt energy transfer in BAM via the formation of color centers.<sup>27</sup> Those authors note that an absorption band appears around 200 nm after VUV irradiation, but no spectra are shown and the data are not discussed any further. The data presented here are in line with those observations.

We believe that the color centers observed here form within the spinel block of the BAM host. First, as noted

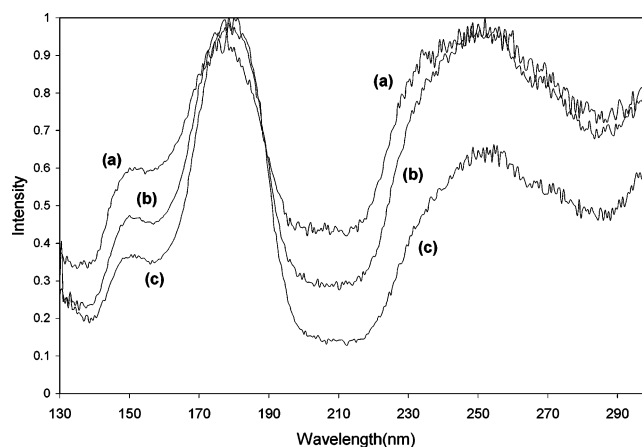


**Figure 7.** Normalized excitation spectra of  $\text{Ba}_{1-x}\text{MgAl}_{10}\text{O}_{17}:\text{Eu}_x$  after 1 h in the VUV life-testing chamber for (a)  $x = 0.10$ , (b)  $x = 0.05$ , and (c)  $x = 0.01$ .

above, excitation into the spinel block (at wavelengths shorter than 160 nm) is more affected by VUV damage, indicating that this is the location of the newly formed electronic defects. We also refer the reader to the data of Gritsyna et al.,<sup>28</sup> who performed a fairly exhaustive study of the relationship between composition and color center formation in spinel,  $\text{MgO} \cdot n\text{Al}_2\text{O}_3$  ( $n = 1\text{--}2.5$ ). They found that UV-irradiation of these materials created several absorption centers, including a prominent absorption between 200 and 300 nm. The intensity of this peak increased as  $n$  increased. Those researchers assigned the absorption centers to antisite defects (e.g.,  $\text{Al}^{3+}$  on an  $\text{Mg}^{2+}$  site). Note that the composition of BAM corresponds to  $n = 5$ , so that there is considerable substitution of  $\text{Al}^{3+}$  for  $\text{Mg}^{2+}$ .<sup>12</sup> Thus, we conclude that the loss of efficiency in VUV-damaged BAM comes from the formation of color centers in the spinel block. These interrupt the radiative transfer of energy from an STE to the activator. In addition, these electronic defects provide traps that also interrupt the nonradiative transfer of energy to  $\text{Eu}^{2+}$ . Finally, some of these color centers absorb at a wavelength (200–300 nm) that is also expected to disrupt the direct excitation of  $\text{Eu}^{2+}$ , as is observed.

Because the energy-transfer mechanism to  $\text{Eu}^{2+}$  depends partly on the excitation wavelength, we also observe spectral differences in how Eu concentration affects the degree of VUV damage. In our discussion, we have proposed three regions of excitation: from 130 to 160 nm, nonradiative excitation of Eu takes place through the spinel block; from 160 to 200 nm, excitation occurs into Ba states, and transfer occurs partially via STE emission; beyond 200 nm, excitation takes place directly at Eu via  $4f^7 \rightarrow 4f^65d$  transitions. Thus, the region between 160 and 200 nm is distinct from the other two in that it has a dependence on the efficiency of STE emission, whereas the other regions have more of a direct dependence on the availability of  $\text{Eu}^{2+}$  states. The effect of this can be seen in Figure 7, in which normalized excitation spectra of VUV-damaged samples with different Eu loadings are presented. In this case, samples were damaged for 1 h in the VUV chamber. As the Eu concentration is increased, we see that the

(28) Gritsyna, V. T.; Afanasyev-Charkin, I. V.; Kobayakov, V. A.; Sickafus, K. E. *J. Am. Ceram. Soc.* **1999**, 82, 3365.

excitation modes that depend more directly on the presence of Eu levels are damaged less relative to excitation that takes place through the STE. Of course, the STE emission must also find Eu atoms in the host for transfer, so that on an absolute scale the efficiency of excitation decreases everywhere. The effect seen in the normalized spectra is therefore a relative one.

### Conclusions

We have studied the optical properties of  $\text{Eu}^{2+}$ -doped and undoped samples of  $\text{BaMgAl}_{10}\text{O}_{17}$ , both before and after irradiation in a custom VUV life-testing chamber. Important conclusions from this work are summarized below.

The color shift observed in VUV-damaged BAM:Eu is attributed to a migration of  $\text{Eu}^{2+}$  ions in the cation layer of the host lattice. Some of the Eu migrates to a metastable defect site that has a fixed concentration and is not available in every unit cell. This site is tentatively associated with O interstitials in the cation layer.

We propose that there are three modes of excitation of  $\text{Eu}^{2+}$  in BAM: (a) excitation wavelengths from 120 to 150 nm promote electrons into mostly spinel-like states. Some of this energy is transferred nonradiatively to  $\text{Eu}^{2+}$ , and some is transferred to Ba states, creating self-trapped excitons. (b) Between 160 and 190 nm,

absorption occurs largely into Ba 5d states, leading to the creation of self-trapped excitons. This exciton emits at 265 nm, providing a means of radiative transfer to  $\text{Eu}^{2+}$ . (c) At wavelengths longer than 200 nm, excitation takes place directly at  $\text{Eu}^{2+}$  ions. There will be overlap between all of these excitation modes, so that the wavelength ranges given here are only rough descriptions of regions where certain processes are dominant.

The primary mechanism for the observed loss of efficiency in these materials is the formation of color centers in the spinel block of the host. These electronic defects provide a nonradiative pathway for the dissipation of absorbed VUV radiation. In addition, these color centers are responsible for the formation of an absorption band at 235 nm that is seen in damaged, undoped materials. This absorption disrupts the radiative energy-transfer mechanism, as well as interrupts the direct excitation of Eu in the ultraviolet.

**Acknowledgment.** We acknowledge Research Corporation Cottrell College Science Awards and OSRAM SYLVANIA, Inc. for funding for this work. We thank Dr. Kerry Hipps and Dr. Ursula Mazur at Washington State University for assistance with the diffuse reflectance measurements.

CM0489284